SEDIMENT FLUX MEASUREMENTS AT A MARS ANALOG SITE. T. N. Titus[1], R. K. Hayward[1], R. Bogle[1] and J. Zimbelman[2],[1]U.S. Geological Survey, Astrogeology Science Center, Flagstaff, AZ (ttitus@usgs.gov) [2]Smithsonian Institution, Washington, D.C.

Introduction: Understanding how the surface and atmosphere interact on Mars is important to the safety of future landed missions, as well as being important to the understanding climate evolution and the potential for past life. Before the repeat coverage of High Resolution Imaging Science Experiment (HiRISE) images, the general scientific consensus was that most, if not all, of the dunes on Mars were immobile. However, recent studies have demonstrated that Martian dunes are changing dramatically in the current climate regime [e.g.,1-6]. Bridges et al. [7] documented dune activity in 23 of 57 repeat HiRISE dune targets, concluding that sand is mobile in virtually all parts of the north polar erg and in many non-polar areas. Sand flux rates measured by Bridges et al. [8] show that flux rates at some places on Mars are similar to flux rates on Earth and that dune fields may have formed in as little as 10,000 years. However, both atmospheric modeling and in situ meteorological measurements on Mars suggest that winds are seldom above the saltation threshold [9-13]. Numerical models and wind tunnel experiments indicate that wind speed needed to keep grains saltating on Mars may be 3 to 10 times less than the wind speed required to initiate saltation [14-15]. The goal of the Grand Falls (GF) project was to measure sediment flux at a Mars analog site and to field test whether hysteresis, the continuation of sand transport by lower velocity winds once saltation has been initiated, can be responsible for the flux rate observed by Bridges et al. [8].

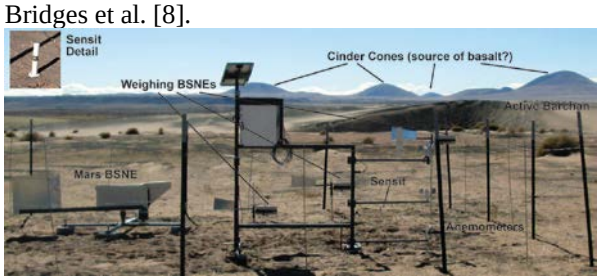

Figure 1: Grand Falls Field Site.

Analog Site: The Grand Falls dune field (~1.6 km x 1 km) is located ~70 km NE of Flagstaff, AZ, and just north of the Little Colorado River (LCR). The dunes at GF are in a relative topographic minimum, migrating toward local topographic maxima that will impede their progress. This setting is analogous to the setting of an estimated 1000 dune fields on Mars that occur within craters and valleys [16-17]. A more detailed description of the analog site can be found in Bogle et al. [18]

Most of the dune sand on Mars is likely of basaltic composition [e.g.,19]. Basalt sand is also present in significant amounts at GF, allowing us to observe its behavior under various atmospheric conditions. Bimodal grain size is another sand characteristic common to both GF and Mars [e.g., 20].

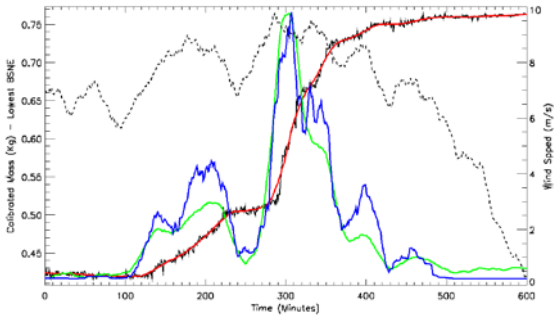

Figure 2: Sediment flux and wind data collected for one 10 hour wind event. The solid black line is the data from the lowest sediment catcher. The red line is the smooth fit to the sediment catcher data. The green line is the gradient of the red line and the blue is the smoothed number of particle impacts from the solid-state saltation sensorS4.

Instrumentation: We installed the following equipment (Figure 1) at GF: one custom-designed sediment sampler, three weighing BSNE (Big Spring Number Eight sediment samplers that passively sample near surface airborne particles and record the weight of the sample at one minute intervals), three anemometers, one directional anemometer, one solid-state saltation sensor (S4), one CR-1000 data logger, two solar panels, and a battery power supply. The equipment has been actively collecting data since November 2013.

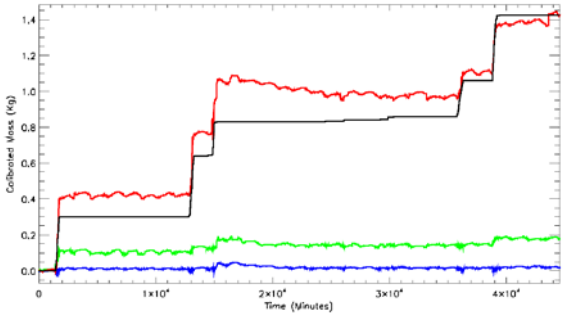

Figure 3: Sediment weight and integrated S4 observations. The red, green, and blue lines are the data from the sediment catchers. The black line is the calibrated data from the S4.

Sediment Flux Calculations: Sediment flux is usually expressed either in units of mass per unit area per unit time (horizontal mass flux (HMF), equation 1)

or as mass per length per unit time (horizontal mass transport (HMT), equation 2) [21]:

$$[1]\ HMF = \dot{q} = \frac{dq}{dt} = {}^{m}/_{At\varepsilon} = \sigma e^{-z/z_0}$$

where m is the sediment mass, A is the areal cross-section of the BSNE opening, t is the integration time, and ε is the BSNE efficiency which is usually 0.4 [22].

If the HMF (q) is measured at multiple heights (z), then an exponential function can be determined where σ is the HMF at one scale height ($z0$).

$$[2]\ HMT = F = \int_0^\infty \dot{q}\ dz = \sigma z_0$$

Equation 1 is the sediment flux through a unit area at a specified height – which is what an individual BSNE measures. Equation 2 is the sediment flux that passes through a horizontal unit length, vertically integrated from ground level to the top of the atmosphere – thus providing an estimate of the total amount of sediment transported by the atmosphere.

Sediment Flux Results from Bulk Samples: Several large wind events have occurred, providing the opportunity to compare wind events. The scale heights of the sediment flux vary little from wind event to wind event, typically ranging between 17 cm and 22 cm. Sediment flux (HMT) appears to be independent of the sediment flux scale height and can vary from 2.6 to 6.7 kg/m/s.

Table 1: Sediment Flux Rates for Selected Wind Events.

Dates	Event Duration (Hrs)	BSNE-1 Mass (Kg)	BSNE-2 Mass (Kg)	BSNE-3 Mass (Kg)	Flux Scale Ht. (m)	HMT (Kg/m/s)
2/28/14	6.3	0.34	0.029	0.0073	0.22	6.7
3/17/14	5.0	0.17	0.020	0.0047	0.27	4.4
4/25/14	8.2	0.13	0.011	0.00	0.16	2.6
5/11/14	9.4	0.35	0.033	0.00	0.17	6.0

Shear Stress Threshold Calculations: By collecting wind speed data at more than one height AGL, we can calculate the shear stress velocity (U^*), by fitting the observations to equation 3.

[3] $U = U^*/k\ ln(z) - U^*/k\ ln(z_0)$,

where k=0.4, z is height, and z_0 is the aerodynamic roughness scale, to find the roughness factor [23]. Once the shear velocity (U*) and surface roughness (z_0) has been determined, wind speed at any height can be interpolated using this same equation. By comparing U^* to the sediment counts from the S4, we can determine $U^*_{initial}$ and $U^*_{continuous}$.

Hysteresis Calculations: Hysteresis analysis cannot be conducted using the sediment catchers. While the sediment catchers provide a measure of the sediment weight each minute, the uncertainty within those measurements due to vibrations, is larger than any increase in sediment mass over a period of a few minutes. Therefore, the only instrument with sufficient signal-to-noise on sediment flux is the S4. Shear stress above 0.6 m/s clearly initiates saltation; however a lower threshold may be possible.

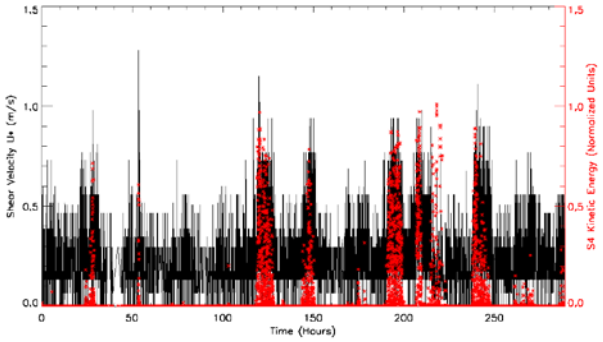

Figure 4: Shear velocity and S4 kinetic energy vs. time. The black lines are the calculated *U over a period of 2 weeks. The red asterisks are the normalized S4 kinetic energy over the same time period. Shear stress above 0.6 m/s clearly initiates saltation; however, a lower threshold may be possible. There are periods when the shear stress should be sufficient to initiate saltation but does not, suggesting that the sediment source may be limited, possibly by environmental factors.**

Acknowledgements: We received MMAMA funding (award number NNH13AV78I) to investigate the role of hysteresis in sediment flux at GF and test a modified sediment sampler for possible use on Mars. We are grateful to the Navajo Nation for allowing us to conduct this experiment on their tribal lands. This project benefits greatly from the efforts of John Vogel and Margaret Hiza.

References: [1] Bourke et al., 2008, *Geomorphology*, **94**, 247-255. [2] Silvestro et al., 2010, *Geophys. Res. Lett.*, **37**, L20203 [3] Chojnacki et al., 2011, *J. Geophys. Res.*, **116**, E00F19 [4] Hansen et al., 2011, *Science*, **331**, 575 [5] Geissler et al., 2010, *J. Geophys. Res.*, **115**, E00F11 [6] Chojnacki et al., 2014, *Icarus*, **232**, 187-219 [7] Bridges et al., 2012a, *Nature*, **485**, 339 [8] Bridges et al., 2012b, *Geology*, **40**, 31. [9] Sullivan et al., 2005, *Nature*, **436**, 58. [10] Greeley et al., 1980, *Geophys. Res. Lett.*, **7**, 121. [11] Hess et al. 1977, *J. Geophys. Res.*, **82**, 4559. [12] Mutch et al., 1976, *Science*, **194**, 87-91. [13] Kok, 2012, *Nature*, **485**, 312-313 [14] Claudin and Andreotti, 2006, *EPSL*, **252**, 30-44. [15] Kok, 2010, *Geophys. Res. Lett.*, **37**, L12202 [16] Hayward et al., 2007, *J. Geophys. Res.*, **112**, E11007 [17] Fenton & Hayward, 2010, *Geomorphology*, **121**, 98. [18] Bogle et al., 2015, *Geomorphology*, **228**, p. 41. [19] Herkenhoff and Vasavada, 1999, *J. Geophys. Res.*, **104**, 16487. [20] Sullivan et al., 2008, *J. Geophys. Res.*, **113**, E06S07 [21] Mendez et al. 2011, *Geomorphology*, **129**, 43-48. [22] Goossens and Offer, 2000, *Atmos. Envir.*, **34**, 1043-1057. [23] von Karman, 1930, *Mechanische Ahnlichkeit und Turbulenz*, Weidmannsche Buchh., Berlin.